ACS APPLIED MATERIALS & INTERFACES

Research Article

www.acsami.org

Optimized Molecular Structure of Photoreactive Biocompatible Block Copolymers for Surface Modification of Metal Substrates

Yasuhiko Iwasaki,*[,†] Akira Matsumoto,[†] and Shin-ichi Yusa[‡]

[†]Department of Chemistry and Materials Engineering, Faculty of Chemistry, Materials and Bioengineering, Kansai University, 3-3-35 Yamate-cho, Suita-shi, Osaka 564-8680, Japan

[‡]Department of Materials Science and Chemistry, Graduate School of Engineering, University of Hyogo, 2167 Shosha, Himeji-shi, Hyogo 671-2280, Japan

Supporting Information

ABSTRACT: Poly(2-methacryloyloxyethyl phosphorylcholine)-*b*-poly(2-methacryloyloxyethyl phosphate-*co*-2-cinnamoyloxyethyl methacrylate) (PMPC-*b*-P(MPA/CMA)) was prepared by reversible addition−fragmentation chain transfer (RAFT)-controlled radical polymerization. The block copolymers were coated on stainless steel (SUS316L) and other metal substrates, and then the surface was subsequently irradiated with UV light. The wettability of a specimen surface treated with a block copolymer was improved in comparison with that of an untreated SUS316L plate. From X-ray photoelectron spectroscopy (XPS) data, it was clear that the P(MPA/CMA) block worked as a binding site on the SUS316L surface. The surface density of the block copolymer-immobilized SUS316L surface was influenced by the molecular weight of the PMPC block. The stability of the immobilized layer was improved by UV irradiation, which induced intermolecular dimerization of the CMA. In addition to the SUS316L surface, various other metal surfaces could be modified by surface immobilization of block copolymers. Serum protein adsorption and fibroblast adhesion were effectively reduced by surface immobilization of block copolymers with optimal molecular weight of PMPC block. The nonfouling property was preserved after 1 week of cell cultivation.

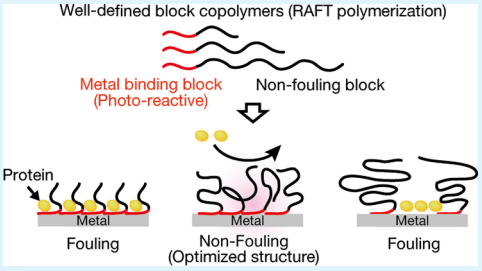

KEYWORDS: *nonfouling, RAFT polymerization, MPC polymer, surface modification, block copolymer, cell adhesion*

INTRODUCTION

Protein adsorption, thrombosis formation, and microbial adhesion, all known as "biofouling," are still serious issues in the development of biomedical devices.[1] Recently, numerous implant materials have been developed that employ the use of various metals.[2] Biofouling presents substantial health risks to patients, often requiring reoperation and replacement of devices as well as incurring considerable costs to the healthcare system.[3] Thus, surface modification to reduce biofouling is necessary to obtain reliable implant materials.[4] Some interesting processes have been developed to create nonfouling surfaces on metal substrates with poly(ethylene oxide)[5−7] and zwitterionic polymers.[8,9] In the current study, we synthesized new block copolymers that can stably attach to metal surfaces and which exhibit excellent protein adsorption- and cell adhesion-resistant properties.

The concept was proposed for making blood-compatible polymer materials that have good stability, processability, and applicability using a methacrylate monomer with a phosphorylcholine group, 2-methacryloyloxyethyl phosphorylcholine (MPC).[10] MPC can polymerize with other vinyl compounds by conventional radical polymerization. The resulting polymers have a surface that resists nonspecific protein adsorption and cell adhesion.[11,12] The use of MPC and MPC polymers to modify the surface properties of polymer materials is a process that is widely used in both research and technology.[13] The coating process is the most appropriate and suitable method for immobilization on various surfaces. Random copolymers of MPC and alkyl methacrylate are normally used for the coating process because the solubility of the MPC copolymer can be controlled by comonomer composition and copolymerization ratio.[11] A surface coated with a copolymer usually has a higher contact angle because the hydrophobic alkyl methacrylates enriched at the air material interface reduce surface free energy. Surface equilibrium with aqueous media is then necessary to orient phosphorylcholine groups at the surface.[14,15] Graft polymerization is another familiar method used to modify surface properties with MPC, and the modified surface is relatively stable because the graft polymers are connected to the substrate by covalent bonding.[16] Graft polymerization can be achieved by several methods such as plasma,[17] corona discharge,[18] photoirradiation,[19,20] etc. Comb-shaped MPC graft polymers at the interface do not need reorientation with aqueous media to exhibit nonfouling properties. As an alternative method, atom transfer radical polymerization (ATRP) of MPC is also applied for surface modification of a solid surface.[21] Although these grafting processes are robust enough to obtain a highly dense graft chain, a reaction chamber or condition for keeping the

Received: April 7, 2012
Accepted: May 29, 2012
Published: May 29, 2012

   dx.doi.org/10.1021/am3006065 | *ACS Appl. Mater. Interfaces* 2012, 4, 3254−3260

process limited is needed for industrial use. Moreover, the surface modification of metal substrates with MPC has not yet been given much study.[22,23]

MPC block copolymers containing photo-cross-linkable phosphate blocks have thus been synthesized for the modification of metal surfaces. It is well-known that phosphate groups can react with the oxidation layer of a metal surface. Textor and co-workers reported that a self-assembled monolayer of dodecyl phosphate and 12-hydroxydodecylphosphate can be generated by the adsorption of alkyl phosphate ammonium salts from an aqueous solution.[24] Phosphoric acid shows a strong affinity to the surfaces of iron oxide nanoparticles through the formation of Fe−O−P bonds, which are more stable than those of carboxylic acid bonds.[25] Surface modification with polymers through a "grafting to" process is good for fabrication, but the low density of the polymers on the surface is sometimes mentioned as a disadvantage of this process. We then synthesized MPC block copolymers with 2-methacryloyoxyethyl phosphate (MPA) through reversible addition−fragmentation transfer (RAFT) polymerization to optimize the molecular structure of the polymers for the sake of efficiency. To obtain a durable polymer on the surface, photo-cross-linkable cinnamoylethyl methacrylate (CMA) was also copolymerized with MPA.

EXPERIMENTS

Materials. SUS316L plate and pure metal foils were purchased from the Nilaco Co., Tokyo, Japan. These metal substrates were cut into 1.2 × 1.2 cm^2 before use. MPC was kindly provided by NOF Co., Ltd. and used without further purification. 4-Cyanopentanoic acid dithiobenzoate was synthesized according to the method reported by McCormick and co-workers.[26] MPA was kindly provided by Unichemical Inc., Nara, Japan and used after removing impurities with hexane. CMA was prepared by a condensation reaction of 2-hydroxyethyl methacrylate and cinnamoyl chloride with triethylamine. The CMA was further purified by silica gel chromatography using chloroform as a mobile phase. Other chemicals were purchased from Wako Pure Chemical Industries, Ltd., Osaka, Japan.

Preparation of Block Copolymers. Poly(MPC)-*b*-poly(MPA-*co*-CMA) (PMPC-*b*-P(MPA/CMA), Figure 1) was

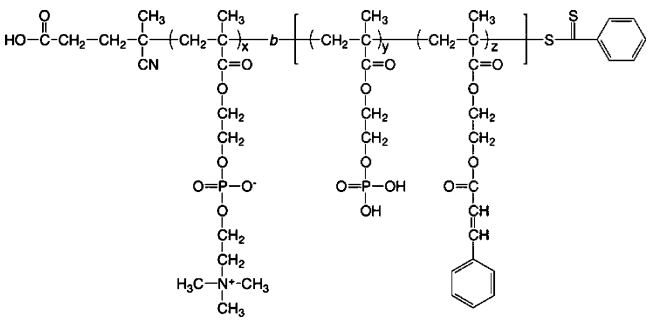

Figure 1. Chemical structure of PMPC-*b*-P(MPA/CMA).

prepared by RAFT polymerization. The reactive condition of the polymerization is summarized in Tables 1 and 2. MPC (10.30 g, 34.88 mmol), 4,4′-azobis(4-cyanopentanoic acid), and 4-cyanopentanoic acid dithiobenzoate were dissolved in methanol, and the volume of the solution was adjusted to 30 mL. Then, to remove oxygen, argon gas was passed through the solution for 30 min. The solution was heated to 70 °C. To remove any unreacted monomer, the solution was dialyzed against pure water for a week and freeze-dried to obtain PMPC-CTA in powder form.

Table 1. Synthetic Results of Macro-CTA

	$[M]_0/[CTA]$	$[CTA]/[I]$	$M_n{}^a \times 10^{-4}$	$M_w/M_n{}^b$	conversion (%)	$M_n{}^c \times 10^{-4}$
$PMPC_{52}$	80	6.9	1.31	1.31	71.5	1.70
$PMPC_{84}$	159	6.9	2.48	1.31	50.4	2.37
$PMPC_{157}$	317	6.9	4.61	1.30	61.0	5.71
$PMPC_{307}$	792	6.9	8.99	1.22	63.8	14.92

[a]Determined by ^{1}H NMR analysis. [b]Determined by GPC measurement. [c]Theoretical molecular weight calculated from $[M]_0/[CTA]$ and conversion.

Table 2. Synthetic Results of Block Copolymers[a]

	$M_n{}^b \times 10^{-4}$	$M_w/M_n{}^c$	conversion (%)	$M_n{}^d \times 10^{-4}$
$PMPC_{52}$-*b*-P(MPA_{33}/CMA_9)	2.48	1.39	20.6	1.76
$PMPC_{84}$-*b*-P(MPA_{28}/CMA_4)	3.14	1.40	73.6	3.27
$PMPC_{157}$-*b*-P(MPA_{24}/CMA_4)	4.93	1.47	62.8	5.28
$PMPC_{307}$-*b*-P(MPA_{32}/CMA_5)	9.81	1.25	62.8	9.66

[a]$[M]_0/[PMPC\text{-}CTA] = 50$; $[PMPC\text{-}CTA]/[I] = 5.0$ [b]Determined by ^{1}H NMR analysis. [c]Determined by GPC measurement. [d]Theoretical molecular weight calculated from $[M]_0/[PMPC\text{-}CTA]$ and conversion.

MPA (0.71 g, 3.38 mmol), CMA (0.10 g 0.38 mmol), 4,4′-azobis(4-cyanopentanoic acid), and PMPC-CTA were dissolved in 30 mL of a cosolvent of ethanol and phosphate buffer solution (pH7.4) (1/1 vol). The solution was deoxygenated by purging with Ar gas for 30 min. Polymerization was performed at 70 °C for 12 h. The block copolymer was purified by dialysis against pure water for a week, changing the pure water twice a day. PMPC-*b*-P(MPA/CMA) was recovered by freeze-drying. Number-average molecular weight (M_n) and molecular weight distribution (M_w/M_n) of MPC-*b*-P(MPA/CMA) were measured with a JASCO GPC system with a refractive index detector and size-exclusion columns, using the PEG standard made up in distilled water containing 10 mM LiBr. The molar contents of the MPA and CMA units in the P(MPA/CMA) block were estimated by ^{1}H NMR. Photodimerization of the cinnamoyl groups of the block copolymers was performed by using an Asahi Spectra MAX-302 equipped with a 300-W Xe lamp and a 275-nm cutoff filter. To monitor the photoreaction of the pendent cinnamoyl groups of PMPC-*b*-P(MPA/CMA), the inner surface of a quartz cell was coated with the polymers and UV−visible absorption was monitored under UV irradiation. The change in the absorption spectra of PMPC-*b*-P(MPA/CMA) coated on the quartz cell during photoirradiation was monitored by UV−visible absorption spectra.

Surface Modification of SUS316L Plate and Other Metal Substrates. Metal plates and foils were soaked overnight in a water−ethanol mixture (1/1 vol) containing 2-wt% of block copolymer. The plates were then rinsed three times with methanol and treated with sonication in methanol for 5 min. The plates were blow dried with N_2 and irradiated with UV light (275 nm) for a given period. The elution test was performed by soaking samples in hot water at 50 °C for 3 h.

Serum Protein Adsorption Test. Uncoated SUS316L plates and polymer-coated SUS316L plates were then soaked in a culture medium (Eagle's MEM; Nissui Pharmaceutical, Tokyo, Japan) containing 10% fetal bovine serum (FBS) at 37 °C. The amount of protein adsorption on the polymer surfaces was determined by the micro-BCA method.[27]

dx.doi.org/10.1021/am3006065 | ACS Appl. Mater. Interfaces 2012, 4, 3254−3260

Cell Culture Experiment. Mouse fibroblasts (L-929 cells) were purchased from RIKEN Cell Bank. The L-929 cells were maintained in a culture medium (Eagle's MEM; Nissui Pharmaceutical, Tokyo, Japan) containing 10% FBS at 37 °C in a humidified atmosphere of air containing 5% CO_2. The contents of the flasks used for cell maintenance were detached by trypsin treatment. Concentration of the L-929 cells was adjusted to 1.0×10^4 cells/mL. The L-929 cells were seeded on sample surfaces and cultured for 20 h in the CO_2 incubator with 95% humidity. After the medium was aspirated, each plate was rinsed three times with PBS and placed in contact with 8 μM Nile Red (Sigma Chemical, St. Louis, MO)/PBS for a few seconds. The plates were then rinsed with PBS and placed in a 2.5-vol% glutaraldehyde solution to fix the adherent cells on the wafer. The wafer was repeatedly rinsed with distilled water and observed with a scanning fluorescence microscope (IX-71, Olympus, Tokyo, Japan). The density of the adherent cells was also measured by lactate dehydrogenase (LDH) assay.[28]

Surface Analysis. Surface composition was measured by X-ray photoelectron spectroscopy (XPS) using an ULVAC-PHI PHI 5000 Versa Probe with Al Kα X-rays. XPS data were collected at various takeoff angles. The dynamic contact angles for the samples were recorded as the probe fluid, water (deionized to 18.2 MΩ), using a First Ten Angstroms FT-125 goniometer and Gilmont syringes. The advancing (θ_A) and receding (θ_R) contact angles were measured with addition to and withdrawal from the drop, respectively.

RESULTS AND DISCUSSION

Synthesis of Block Copolymers. Yusa and co-workers performed homopolymerization of MPC by the RAFT process employing 4,4′-azobis(4-cyanopentanoic acid) as a water-soluble initiator and 4-cyanopentanoic acid dithiobenzoate as a water-soluble chain transfer agent (CTA).[29] The RAFT polymerization of MPC in aqueous solution was rapid at 70 °C; monomer conversions of 90 and 99.4% were reached within 60 and 240 min, respectively. Even though polymerization was rapid, "living" polymerization was confirmed by the fact that monomer consumption followed first-order kinetics while the distribution of molecular weight remained narrow.

The synthetic results of the block copolymer (PMPC-*b*-P(MPA/CMA)) are listed in Tables 1 and 2. We synthesized PMPC having four different molecular weights by changing the ratio of $[M]_0/[\mathrm{CTA}]$. Although the difference of the experimental and theoretical molecular weights of PMPC was increased with an increase in the $[M]_0/[\mathrm{CTA}]$ ratio, the range of molecular weight was relatively narrow ($M_w/M_n \approx 1.3$). Block copolymers were synthesized using PMPCs as macro chain transfer agents (PMPC-CTA). The molecular weight of the block copolymers coincided well with the theoretical amount, which was calculated from the ratio of $[M]_0/[\mathrm{PMPC\text{-}CTA}]$ and conversion. Copolymerization of MPA and CMA using PMPC-CTA proceeded in a "living" manner. The monomer consumption followed first-order kinetics (See the Supporting Information, Figure S1). The semilogarithmic plot indicates that polymerization is first order with respect to the monomer and implies that the polymer radical concentration remains constant on the polymerization time scale.

Controlled polymerization of MPA with RAFT polymerization was performed by Suzuki et al.[30] They used methanol as the polymerization solvent. However, in this study, methanol could not be used because hydrolysis of 4-cyanopentanoic acid dithiobenzoate occurred due to acidic MPA. To reduce the hydrolysis of the dithioester in contact with the acidic monomer, a mixed solvent of methanol and PBS was used to adjust the pH of the polymerization medium to 7.4. Suzuki and co-workers also reported that gelation of MPA occurred when the molecular weight exceeded 20K.[30] They determined the gelation mechanism of phosphate monomers by hydrolysis of the polymers under basic conditions. Most, if not all, cross-linking of MPA is through the side chain and not through the polymer backbone. In this case, cross-linking is inversely dependent upon the chain length of the polymer: the greater the chain length, the greater the conditional probability for cross-linking. We then controlled the molecular weights of P(MPA/CMA) to be less than 10K to reduce gelation. All block copolymers could be well-solved in aqueous media.

Surface Modification and Characterization of Metal Substrates with Block Copolymers. All block copolymers were dissolved in a cosolvent of water and ethanol (1/1 vol). Figure 2a shows the UV−visible absorption spectra for the

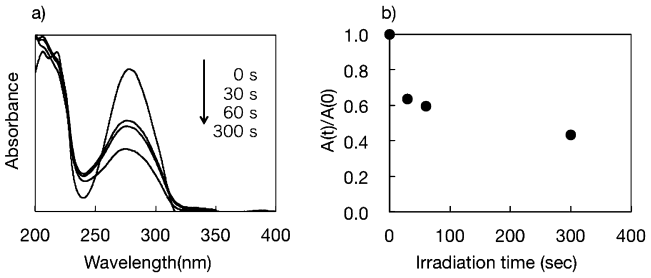

Figure 2. (a) Change in absorption spectra of $PMPC_{157}$-*b*-P(MPA_{24}/CMA_4) coated on a quartz cell after UV irradiation. (b) Plots of $A(t)/A(0)$ versus UV irradiation time.

$PMPC_{157}$-*b*-P(MPA_{24}/CMA_4) coated on the inner surface of a quartz cell upon irradiation of UV light. In the UV−visible absorption spectra, the CMA unit in $PMPC_{157}$-*b*-P(MPA_{24}/CMA_4) exhibits an absorption peak centered at 279 nm, characteristic of the cinnamoyl group. The absorbance decreases progressively with UV irradiation time. This decrease in absorbance is caused by trans-to-cis photoisomerization and [2 + 2] photocycloaddition reactions of the cinnamoyl groups. Progress of the photoreaction (A(t)/A(0)) of the pendant cinnamoyl groups with UV irradiation time is plotted in Figure 2b, where $A(t)$ and $A(0)$ are the absorbances at 279 nm at irradiation time t and 0 min, respectively. It appears that the change in the absorption spectrum occurred remarkably within 30 s.

Metal substrates were soaked in the solution overnight at room temperature. It is well-known that phosphoric acid moieties interact exclusively with surface hydroxyl or coordinatively unsaturated surface metal atoms of metal oxides to form P−O-M bonds. The interaction even works in protic solvents such as alcohol and alcohol−water mixtures, i.e., there is no need for a harmful organic solvent.[24] Molecules having a phosphate group are also widely used as moisture corrosion inhibitors for metal surfaces.[31] For this application, the metal surfaces are normally treated with the inhibitors from an aqueous medium.

Figure 3 and Table 3 show the effect of UV irradiation on the stability of immobilized polymers on a SUS316L surface. The periods of UV irradiation influenced the loss % of XPS P/Fe ratio, as shown in Figure 3. For the first 30 s of irradiation, the loss % decreased with an increase in irradiation time, but the loss % began to increase after 30 s of irradiation. Although dimerization

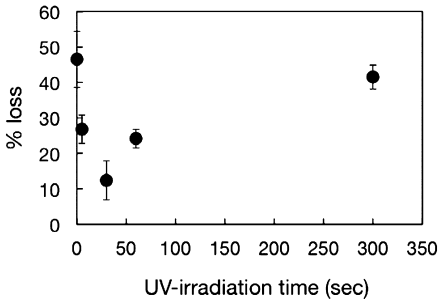

Figure 3. Effect of UV irradiation time on % loss of P/Fe (●) for $PMPC_{157}$-*b*-P(MPA_{24}/CMA_4) coated SUS316L through elution test. The takeoff angle of XPS was adjusted to 45°. Data for each sample was taken from four different substrates, after which they were expressed as the arithmetic mean ± standard deviation (SD).

of CMA increased with an increase in the UV irradiation period, excess UV irradiation induced elution of polymers from the substrate. Photoinduced degradation of polymers by 300 s of UV irradiation was not recognized by using GPC and ^{1}H NMR analyses. On the contrary, an increment in the molecular weight of polymers caused by UV irradiation was observed in the 2.0-w% aqueous solution (see the Supporting Information, Figure S2). The exact mechanism for the increment of polymer elution via longer-term photoirradiation has not yet been clarified but it can be considered that photo-oxidation might influence the P−O−M bonds generated between the SUS316 surface and the immobilized polymers.

Table 3 summarizes XPS atomic ratios (N/Fe) for polymer-coated SUS316L and shows the effect of UV irradiation (30 s) on immobilization stability. XPS N_{1s} spectra of polymer−coated SUS316L after elution test are shown in the Supporting Information, Figure S3. The N/Fe ratio increased with an increase in the chain length of PMPC until the polymerization degree of MPC was 84 and the ratio then became a plateau until the degree was 157. In contrast, the N/Fe ratio decreased a great deal when the polymerization degree of MPC was 307. A similar tendency was observed for the P/Fe ratio (data not shown). Steric hindrance of high molecular weight PMPC chains influence the density of block copolymers immobilized on the surface. After the elution test, approximately 40−50% of the N/Fe ratio was decreased in every sample without UV irradiation. The effect of UV irradiation on reducing polymer elution was also observed. In particular, the coating stability of the block copolymers having low-molecular-weight PMPC was greatly improved. It could also be considered that the surface density of $PMPC_{307}$-*b*-P(MPA_{32}/CMA_5) might be too low to form intermolecular cross-linking networks.

To clarify the effect of PMA units on polymer attachment to a SUS316L surface, $PMPC_{157}$-*b*-$PCMA_{13}$ was synthesized and treated with a similar procedure. As shown in Table 3, the N/Fe ratio of $PMPC_{157}$-*b*-$PCMA_{13}$ was extremely low in comparison with that of $PMPC_{157}$-*b*-P(MPA_{24}/CMA_4) regardless of UV irradiation.

Furthermore, the orientation of $PMPC_{157}$-*b*-P(MPA_{24}/CMA_4) was determined by angle-resolved XPS (ARXPS). Figure 4

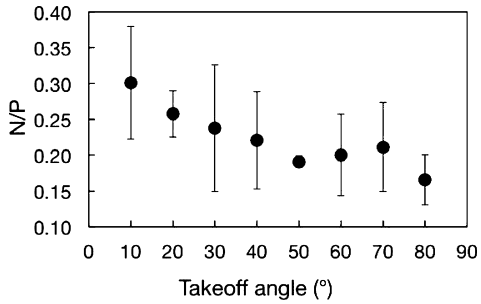

Figure 4. Angle-resolved XPS (ARXPS) N/P ratio of SUS316L surface coated with $PMPC_{157}$-*b*-P(MPA_{24}/CMA_4). Data for each sample was taken from four different substrates, after which they were expressed as the arithmetic mean ± standard deviation (SD).

shows the ARXPS N/P ratio of the SUS316L surface coated with $PMPC_{157}$-*b*-P(MPA_{24}/CMA_4). The ratio was gradually decreased with an increase in the takeoff angles and became a plateau from 50° to 80°. The obtained ARXPS data for the MPC_{157}-*b*-P(MPA_{24}/CMA_4) layer on the SUS316L surface suggested a decrease in the number of phosphorus atoms at the upper level of the constructed polymer layer. The results shown in Table 3 and Figure 4 indicate that the phosphorus content was enriched at the interface of the polymer and SUS316, that is, the block copolymers bind to the surface via MPA units.

Table 4 summarizes XPS atomic compositions and water contact angle data of the metal substrates that were immobilized with $PMPC_{157}$-*b*-P(MPA_{24}/CMA_4). Before each measurement, each specimen was soaked in hot water at 50 °C for 3 h. The signals of N_{1s} at 404 eV and P_{2p} at 135 eV were not observed from any specimens before surface immobilization with the polymers. The water contact angle data was recorded using specimens dried for several hours under reduced pressure before measurement. For all metal substrates, the water contact angle data was decreased by immobilization with $PMPC_{157}$-*b*-P(MPA_{24}/CMA_4). In addition, the θ_A and θ_R on the surfaces coated with the block copolymers were similar values regardless of the type of metal. These surface analyses demonstrated that $PMPC_{157}$-*b*-P(MPA_{24}/CMA_4) coating is able to form on metals with native oxide surfaces (SUS316L, Ti, Mo, Nb, and Cu) and even noble metal (Ag).

Protein Adsorption and Cell Adhesion. Figure 5 shows the amount of protein adsorption on polymer-immobilized

Table 3. XPS Atomic Ratios of Polymer-Coated SUS316L before and after Elution Test

	N/Fe[a] (nonirradiation)			N/Fe[a] (30 s UV irradiation)		
elution test	before[b]	after[b]	% loss	before[b]	after[b]	% loss
$PMPC_{52}$-*b*-P(MPA_{33}/CMA_9)	1.19 (0.05)	0.71 (0.07)	40.3	1.17 (0.19)	1.09 (0.11)	6.8
$PMPC_{84}$-*b*-P(MPA_{28}/CMA_4)	1.66 (0.05)	0.90 (0.12)	45.7	1.57 (0.20)	1.37 (0.25)	12.7
$PMPC_{157}$-*b*-P(MPA_{24}/CMA_4)	1.33 (0.22)	0.90 (0.20)	33.1	1.62 (0.19)	1.28 (0.21)	21.0
$PMPC_{307}$-*b*-P(MPA_{32}/CMA_5)	0.92 (0.07)	0.51 (0.19)	44.6	1.11 (0.13)	0.58 (0.09)	47.7
$PMPC_{157}$-*b*-$PCMA_{13}$		0.24 (0.02)			0.26 (0.04)	

[a]Takeoff angle of XPS analyses was adjusted to 45°. [b]Data for each sample was taken from four different substrates, after which they were expressed as the arithmetic mean ± standard deviation (SD).

Table 4. XPS Atomic Composition and Water Contact Angle Data of $PMPC_{157}$-*b*-P(MPA_{24}/CMA_4)-Coated Metal Substrates after Elution Test

substrate	XPS atomic composition[a,b]	water contact angle (deg)[a] θ_A	θ_R
SUS316L	$C_{49.6}O_{39.3}N_{1.9}P_{3.6}Fe_{1.8}Cr_{3.2}Ni_{0.5}$	41	14
Ti	$C_{49.9}O_{39.8}N_{2.3}P_{3.5}Ti_{4.5}$	32	14
Mo	$C_{44.5}O_{46.0}N_{1.5}P_{2.9}W_{5.2}$	43	13
Nb	$C_{51.0}O_{37.4}N_{2.7}P_{3.6}Nb_{5.8}$	28	13
Cu	$C_{43.7}O_{39.8}N_{1.7}P_{2.4}Cu_{11.6}$	34	13
Ag	$C_{63.4}O_{26.6}N_{2.4}P_{3.7}Ag_{3.9}$	41	18

[a]Each substrate was treated with UV light for 30 s before elution test. [b]Determined using 45° takeoff angle data.

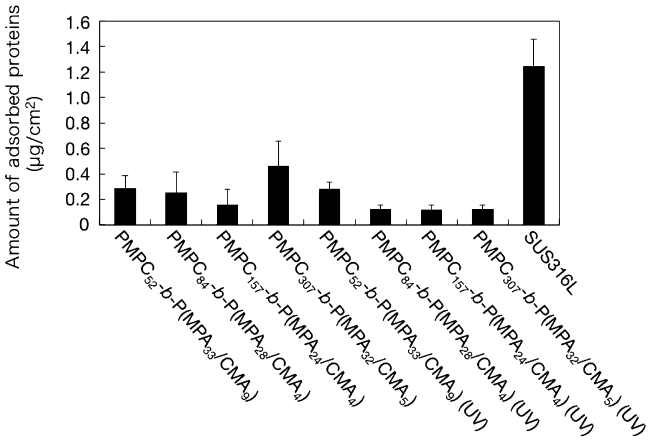

Figure 5. Amount of protein adsorbed on SUS316L surface immobilized with block copolymers after contact with 10% bovine serum for 3 h. The amount of adsorbed protein on every polymer-immobilized surface was significantly lower ($p < 0.01$) than that on the SUS316 surface. Data for each sample was taken from four different substrates, after which they were expressed as the arithmetic mean ± standard deviation (SD).

SUS316L surfaces after contact with 10% fetal bovine serum at 37 °C for 3 h. On the SUS316L surface, a large amount of serum proteins was adsorbed. In contrast, surfaces immobilized with block copolymers showed significantly reduced serum protein adsorption. In particular, the amount of protein on $PMPC_{84}$-*b*-P(MPA_{28}/CMA_4) and $PMPC_{157}$-*b*-P(MPA_{24}/CMA_4) was almost suppressed. These polymer surfaces have a high N/Fe ratio, as shown in Table 3. Feng et al. reported that the effects of thickness and density of PMPC polymer on protein adsorption is well characterized.[32] Surface samples with various graft densities from 0.06 to 0.39 chains/nm^2 and chain lengths from 5 to 200 MPC units were prepared via the "grafting from" process. They clarified that surfaces with high graft densities and high PMPC chain lengths showed dramatic reductions in fibrinogen adsorption. In this study, we applied the "grafting to" process for surface modification. The grafting density of the block copolymers must be much less ($\ll$0.1) than that of the dense polymer brushes generated by the "grafting from" process.[33] However, protein adsorption was effectively reduced on block copolymer-immobilized surfaces. Yoshimoto and co-workers compared the nonfouling characteristics of PMPC- and PEG-modified gold surface.[34] They clarified that the number of MPC units on the gold surface appears to be an important factor in the excellent protein resistance offered by PMPC-modified gold surfaces fabricated by the "grafting to" method, which is in sharp contrast to that of PEG tethered chains. Optimization of the chain length of block copolymers is important for enriching the number of MPC units on the surface; RAFT polymerization was quite useful for controlling polymer structure.

UV irradiation on a polymer-immobilized surface also influenced the reduction of protein adsorption because of the stabilization of the polymer layer on SUS316L. It is well-known that protein adsorption is strongly related to biofouling by body fluids. Biofouling is a trigger for contamination, thrombus formation, infection, adhesion, etc. Reduction of nonspecific protein adsorption is a basic requirement for the surfaces of biomedical materials. MPC block copolymers are effective for generating a suitable surface on metal biomaterials.

Adhesion of L929 was determined for 4 and 7 days of cultivation. In general, the cell adhesion resistance of MPC polymer has been investigated under short-term cultivation.[18,35] Tugulu et al., reported that dense PEG brushes were found to detach from the substrates upon prolonged exposure to cell culture medium.[36] This release of PEG brushes from the substrates is due to osmotic stress, which adds to the entropically unfavorable stretched chain conformation at high brush densities and facilitates cleavage of the chemical bond that links the polymer brush to the substrate. Cleavage of the polymer brush results in an increase in nonspecific protein adsorption and cell adhesion. We have now investigated the nonfouling properties of block-copolymer-immobilized surfaces for 4 and 7 days of cell cultivation. Figure 6 shows fluorescence micrographs of SUS316L and that immobilized with $PMPC_{157}$-*b*-P(MPA_{24}/CMA_4) after cultivation of L929 cells for 7 days. Many adherent cells were observed on the SUS316L surface, but cell

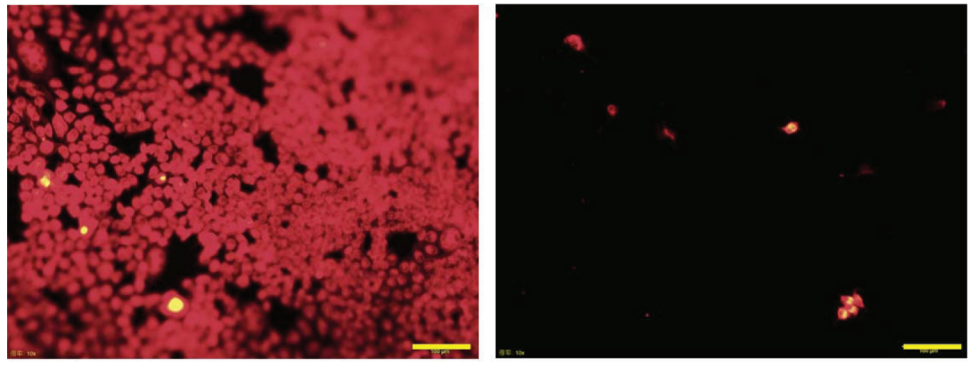

Figure 6. Fluorescence micrographs of SUS316L surface and $PMPC_{157}$-*b*-P(MPA_{24}/CMA_4)-immobilized surface after cultivation of L929 cells for 7 days. Scale bars represent 100 μm.

adhesion was effectively reduced on surfaces treated with $PMPC_{84}$-*b*-$P(MPA_{28}/CMA_4)$ or $PMPC_{157}$-*b*-$P(MPA_{24}/CMA_4)$. The effect of the molecular structure of immobilized polymers on cell adhesion is summarized in Figure 7. Similar to the results with

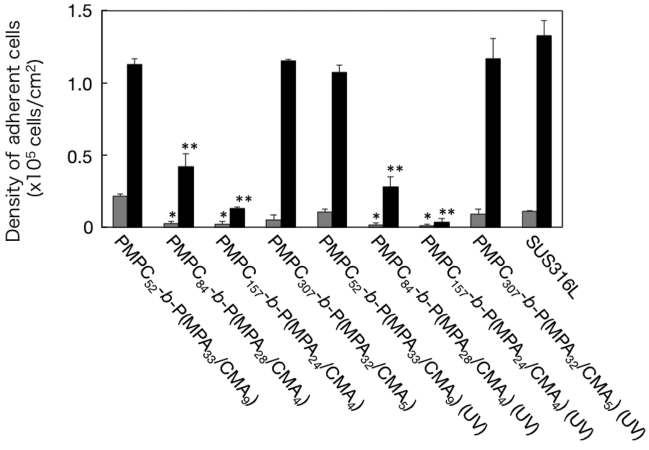

Figure 7. Density of adherent L929 cells on SUS316L surface immobilized with block copolymers after 4 (grey) and 7 (black) days of cultivation. Data for each sample was taken from four different substrates, after which they were expressed as the arithmetic mean ± standard deviation (SD). *p < 0.01 vs SUS316L(4-days cultivation), **p < 0.01 vs SUS316L(7-days cultivation).

protein adsorption, cell adhesion was significantly reduced on surfaces treated with $PMPC_{84}$-*b*-$P(MPA_{28}/CMA_4)$ or $PMPC_{157}$-*b*-$P(MPA_{24}/CMA_4)$. As shown in Table 3, the N/Fe ratio of $PMPC_{52}$-*b*-$P(MPA_{33}/CMA_9)$- and $PMPC_{307}$-*b*-$P(MPA_{32}/CMA_5)$-immobilized surfaces was relatively low and the density of MPC units on the surface might not be sufficient to reduce cell adhesion. Furthermore, the reduction of adherent cells on $PMPC_{84}$-*b*-$P(MPA_{28}/CMA_4)$- and $PMPC_{157}$-*b*-$P(MPA_{24}/CMA_4)$- immobilized surfaces after 7 days cultivation was further improved with UV-treatment of the substrates. It was shown that the coating durability of these block copolymers on metal surfaces was raised with cross-linking of the CMA units in the block copolymers.

CONCLUSION

In this paper, we synthesized photoreactive MPC block copolymers with MPA, which act as anchors on metal surfaces. The block copolymers can be processed with aqueous solutions and successfully attached to various metal surfaces. By XPS analysis, it was clarified that the MPA units were important for obtaining a reliable polymer coating of metal surfaces. Resistance to biofouling on polymer-immobilized surfaces strongly depends on the molecular weight of the PMPC segment. Dimerization of the cinnamoyl groups in the phosphate segment improved the stability of the immobilization layer on metal surfaces and the nonfouling properties were well preserved after one week of cell cultivation. By using controlled radical polymerization, we were able to optimize the molecular structure of MPC block copolymers for improving the nonfouling properties of metal surfaces.

ASSOCIATED CONTENT

Supporting Information

Additional figures showing polymerization kinetics, photoreactivity of a block copolymer, and XPS spectra. This material is available free of charge via the Internet at http://pubs.acs.org.

AUTHOR INFORMATION

Corresponding Author

*E-mail: yasu.bmt@kansai-u.ac.jp. Telephone: +81-6-6368-0900. Fax: +81-6-6368-0900.

Notes

The authors declare no competing financial interest.

ACKNOWLEDGMENTS

This study was supported by the Adaptable and Seamless Technology Transfer Program through Target-driven R&D, JST (11-128) and MEXT-Supported Program for the Strategic Research Foundation at Private University, 2009-2014.

REFERENCES

(1) Castner, D. G.; Ratner, B. D. *Surf. Sci.* **2002**, *500*, 28−60.
(2) Katti, K. S. *Colloid. Surface B* **2004**, *39*, 133−142.
(3) Vasilev, K.; Cook, J.; Griesser, H. J. *Expert Rev. Med. Devices* **2009**, *6*, 553−567.
(4) Hendricks, S. K.; Kwok, C.; Shen, M.; Horbett, T. A.; Ratner, B. D.; Bryers, J. D. *J. Biomed. Mater. Res.* **2000**, *50*, 160−170.
(5) Yoshimoto, K.; Nozawa, M.; Matsumoto, S.; Echigo, T.; Nemoto, S.; Hatta, T.; Nagasaki, Y. *Langmuir* **2009**, *25*, 12243−12249.
(6) Khoo, X.; Hamilton, P.; O'Toole, G. A.; Snyder, B. D.; Kenan, D. J.; Grinstaff, M. W. *J. Am. Chem. Soc.* **2009**, *12* (131), 10992−10997.
(7) Gillich, T.; Benetti, E. M.; Rakhmatullina, E.; Konradi, R.; Li, W.; Zhang, A.; Schlüter, A. D.; Textor, M. *J. Am. Chem. Soc.* **2011**, *133*, 10940−10950.
(8) Li, G.; Xue, H.; Cheng, G.; Chen, S.; Zhang, F.; Jiang, S. *J. Phys. Chem. B.* **2008**, *112*, 15269−15274.
(9) Ye, S. H.; Johnson, C. A., Jr.; Woolley, J. R.; Snyder, T. A.; Gamble, L. J.; Wagner, W. R. *J. Biomed. Mater. Res. A* **2009**, *91*, 18−28.
(10) Ishihara, K.; Ueda, T.; Nakabayashi, N. *Polym. J.* **1990**, *22*, 355−360.
(11) Ishihara, K.; Nomura, H.; Mihara, T.; Kurita, K.; Iwasaki, Y.; Nakabayashi, N. *J. Biomed. Mater. Res.* **1998**, *39*, 323−330.
(12) Ueda, T.; Oshida, H.; Kurita, K.; Ishihara, K.; Nakabayashi, N. *Polym. J.* **1992**, *24*, 1259−1269.
(13) Iwasaki, Y.; Ishihara, K. *Anal. Bioanal. Chem.* **2005**, *381*, 534−546.
(14) Lewis, A. L.; Hughes, P. D.; Kirkwood, L. C.; Leppard, S. W.; Redman, R. P.; Tolhurst, L. A.; Stratford, P. W. *Biomaterials* **2000**, *21*, 1847−1859.
(15) Iwasaki, Y; Yamasaki, A; Ishihara, K. *Biomaterials* **2003**, *24*, 3599−3604.
(16) Ishihara, K.; Nakabayashi, N.; Fukumoto, K.; Aoki, J. *Biomaterials* **1992**, *13*, 145−149.
(17) Hsiue, G. H.; Lee, S. D.; Chang, P. C. T.; Kao, C. Y. *J. Biomed. Mater. Res.* **1998**, *42*, 134−147.
(18) Iwasaki, Y.; Sawada, S.; Nakabayashi, N.; Khang, G.; Lee, H. B.; Ishihara, K. *Biomaterials* **1999**, *20*, 2185−2191.
(19) Ishihara, K.; Iwasaki, Y.; Ebihara, S.; Shindo, Y.; Nakabayashi, N. *Colloids Surf., B* **2000**, *18*, 325−335.
(20) Kyomoto, M.; Ishihara, K. *ACS Appl. Mater. Interfaces* **2009**, *1*, 537−542.
(21) Iwata, R.; Suk-In, P.; Hoven, V. P.; Takahara, A.; Akiyoshi, K.; Iwasaki, Y. *Biomacromolecules* **2004**, *5*, 2308−2314.
(22) Kyomoto, M.; Moro, T.; Iwasaki, Y.; Miyaji, F.; Kawaguchi, H.; Takatori, Y.; Nakamura, K.; Ishihara, K. *J. Biomed. Mater. Res.* **2009**, *91A*, 730−741.
(23) Yao, Y.; Fukazawa, K.; Huang, N.; Ishihara, K. *Colloids Surf., B* **2011**, *88*, 215−220.
(24) Tosatti, S.; Michel, R.; Textor, M.; Spencer, N. D. *Langmuir* **2002**, *18*, 3537−3548.
(25) Sahoo, Y.; Pizem, H.; Fried, T.; Golodnitsky, D.; Burstein, L.; Sukenik, N. C.; Markovich, G. *Langmuir* **2001**, *17*, 7907−7911.
(26) Mitsukami, Y.; Donovan, M. S.; Lowe, A. B.; McCormick, C. L. *Macromolecules* **2001**, *34*, 2248−2256.

(27) Iwasaki, Y.; Fujiike, A.; Kurita, K.; Ishihara, K.; Nakabayashi, N. *J. Biomater. Sci. Polym. Ed* **1996**, *8*, 91−102.
(28) Iwasaki, Y.; Takami, U.; Shinohara, Y.; Kurita, K.; Akiyoshi, K. *Biomacromolecules* **2007**, *8*, 2788−2794.
(29) Yusa, S.; Fukuda, K.; Yamamoto, T.; Ishihara, K.; Morishima, Y. *Biomacromolecules* **2005**, *6*, 663−670.
(30) Suzuki, S.; Whittaker, M. R.; Grøndahl, L.; Monteiro, M. J.; Wentrup-Byrne, E. *Biomacromolecules* **2006**, *7*, 3178−3187.
(31) Ahearn, J. S.; Davis, G. D.; Sun, T. S.; Venables, J. D. In *Adhesion Aspects of Polymeric Coatings*; Mittal, K. L., Ed.; Plenum Press: New York, 1983; p 281.
(32) Feng, W.; Brash, J. L.; Zhu, S. *Biomaterials* **2006**, *27*, 847−855.
(33) Tsujii, Y.; Ohno, K.; Yamamoto, S.; Goto, A.; Fukuda, T. *Adv. Polym. Sci.* **2006**, *197*, 1−45.
(34) Yoshimoto, K.; Hirase, T.; Madsen, J.; Armes, S. P.; Nagasaki, Y. *Macromol. Rapid Commun.* **2009**, *30*, 2136−2140.
(35) Ishihara, K.; Ishikawa, E.; Iwasaki, Y.; Nakabayashi, N. *J. Biomater. Sci. Polym. Ed.* **1999**, *10*, 1047−1061.
(36) Tugulu, S.; Klok, H. A. *Biomacromolecules* **2008**, *9*, 906−912.